Forecasting the Disturbed Storm Time Index

Charles J. Wetterer

Pacific Defense Solutions, LLC

CONFERENCE PAPER

The Disturbed Storm Time (Dst) index is a measure of the magnetic field (in nT) created by the ring current, an electric current carried by charged particles trapped in the Earth's magnetosphere. The index is calculated from measurements at 4 magnetometer stations near the equator and referenced to zero on "internationally designated quiet days." As with other geomagnetic indices, the Dst index exhibits a high degree of correlation from one value to the next. In fact, existing forecast models that strictly use solar wind and interplanetary magnetic field data as inputs have a difficult time matching the performance of simple persistence when evaluating the model by the linear correlation coefficient and the root mean square error between forecast values and actual values. A model using the unscented Kalman filter (UKF) as the forecast engine was developed in an attempt to improve on simple persistence and existing models. This UKF model is very similar to the model we used to forecast the planetary geomagnetic index (Kp) last year (*Wetterer et al.* [2010]) that outperformed all other existing Kp forecast models. Initial results using this UKF forecast model to forecast Dst shows a similar performance and are detailed in this paper. The UKF-based model offers the opportunity for further forecast improvement by adding new inputs and refining the state and measurement functions in the filter.

1. INTRODUCTION

The Disturbed Storm Time (*Dst*) index is one of the commonly used geomagnetic indices to indicate the severity of global magnetic disturbances. It is a measure of the magnetic field (in nT) created by the ring current caused by trapped particles around the Earth. Specifically, hourly values are derived from measurements by 4 magnetometer stations (Figure 1) near the equator and referenced to zero on "internationally designated quiet days." The World Data Center for Geomagnetism, Kyoto (http://wdc.kugi.kyoto-u.ac.jp/dst_realtime/presentmonth/index.html) provides a near real-time "Quicklook" value, a provisional value after approximately two years, and a final value after approximately six years.

Fig. 1. Magnetometer stations used to calculate various geomagnetic indicies: Polar Cap (PC) – red, Auroral Electroject (AE) – green, Planetary Geomagnetic (Kp) – purple, Disturbed Storm Time (Dst) - blue.

Last year we used the unscented Kalman filter (UKF) as the engine behind forecasting the planetary geomagnetic index, Kp. The resulting forecasts had a higher correlation and lower root-mean square error between forecast values and actual values than all previously published forecast models. This paper again uses the UKF as the forecast engine, but this time for the *Dst* index. As with our previous paper, we will first use simple persistence as a forecast model to establish a baseline and then compare the performance of the UKF-based forecast model to this baseline and previously published empirical neural network-based forecast models.

2. THE *Dst* SIMPLE PERSISTENCE MODEL

The hourly *Dst* index values were tabulated using the archives at the World Data Center for Geomagnetism, Kyoto (http://swdcwww.kugi.kyoto-u.ac.jp/index.html). Fig. 2 displays the frequency distribution of *Dst* during the period covered (1957-2006). *Dst* < -65 nT is considered storm-time values and occur infrequently compared to the quiet day values of *Dst* ≈ 0 nT.

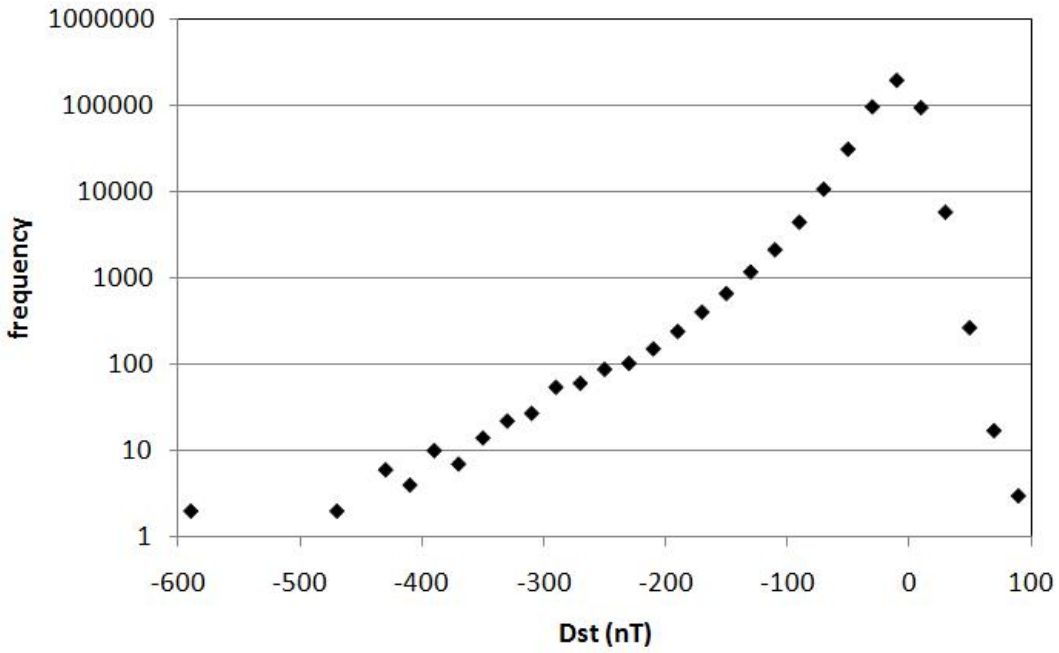

Fig. 2 – Frequency distribution of Dst values for 1957-2006.

A forecast model based on the nowcast *Dst* will be evaluated to form a baseline to compare all other forecast models. Three measures will be used to measure the performance of the forecast models: linear correlation between the forecast values and actual values (Eq. 1), root-mean square error (RMSE) between the forecast values and actual values (Eq. 2), and the storm-onset Heidke Skill Score (Eq. 3).

$$r = \frac{n\sum_i Dst_i^a Dst_i^f - \sum_i Dst_i^a \sum_i Dst_i^f}{\sqrt{n\sum_i \left(Dst_i^a\right)^2 - \left(\sum_i Dst_i^a\right)^2}\sqrt{n\sum_i \left(Dst_i^f\right)^2 - \left(\sum_i Dst_i^f\right)^2}} \quad (1)$$

$$RMSE_{Dst} = \sqrt{\frac{\sum_i \left(Dst_i^a - Dst_i^f\right)^2}{n}} \quad (2)$$

where Dst^a are actual *Dst* values, Dst^f are forecast values, and n is the number of actual *Dst* values.

$$SS = \frac{2(ad - bc)}{(a+c)(c+d)+(a+b)(b+d)} \tag{3}$$

where it is calculated only when a "storm threshold" is reached and where (a) is when $Dst^a_{i+1} \geq Dst^a_i + T$ and $Dst^f_{i+1} \geq Dst^f_i + T - S$, a "miss" (c) is when $Dst^a_{i+1} \geq Dst^a_i + T$ and $Dst^f_{i+1} < Dst^f_i + T + S$, a "false positive" (b) is when $Dst^a_{i+1} < Dst^a_i + T$ and $Dst^f_{i+1} \geq Dst^f_i + T - S$, and a "correct rejection" (d) is when $Dst^a_{i+1} < Dst^a_i + T$ and $Dst^f_{i+1} < Dst^f_i + T + S$, *T* is an "increase threshold" corresponding to the change in *Dst* required for the onset of a geomagnetic storm and *S* is a "tolerable error" in forecasting the magnitude of the onset. By this measure, simple persistence will always have a storm onset skill score of SS = 0, for storm threshold of *Dst* = -65 nT, *T* = -10 nT, and *S* = -3 nT.

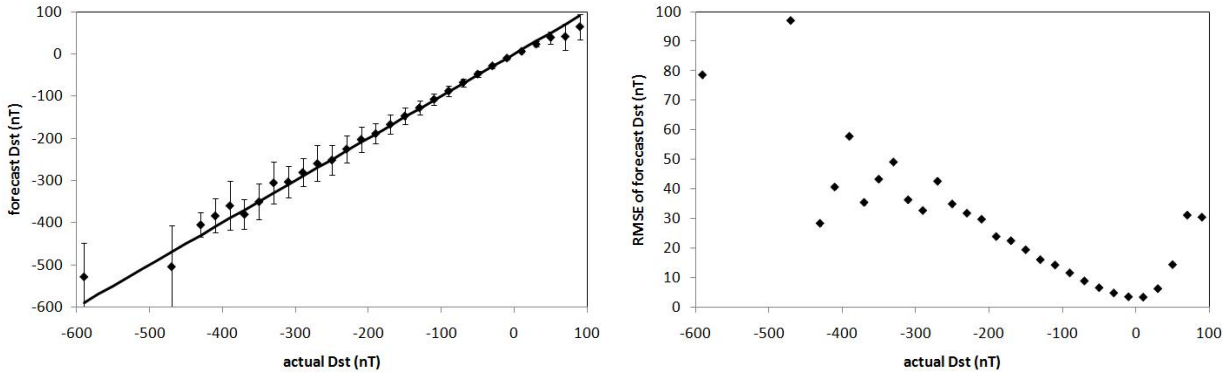

Fig. 3 –*Dst* simple persistence model 1-hour ahead performance. (a) predicted versus actual and (b) RMSE

Fig. 3a shows the forecast versus actual results of running the models on all the data (1 hour time interval) to provide a forecast 1 hour ahead. The linear correlation coefficient is 0.979. Fig. 3b shows the root-mean square error (RMSE) in the predicted values as a function of the actual *Dst* values. The average RMSE is 5.09 nT. The high correlation coefficient and relatively low RMSE is due to the preponderance of *Dst* values near quiet-time and low frequency of storm-time values.

3. PREVIOUS FORECAST MODELS

Burton et al. [2] developed an empirical function to calculate the Dst index based on measurements of the solar wind and interplanetary magnetic field (Eqs. 4-7).

$$\frac{dDst^*}{dt} = \alpha(t)(\varepsilon(t) - \mathrm{E}) - \frac{Dst^*}{\tau(t)} \tag{4}$$

where

$$Dst^* = Dst - b(P_{dyn})^{1/2} + c \tag{5}$$

$$\varepsilon(t) = v_x(t) B_z(t) \tag{6}$$

$$P_{dyn}(t) = n(t) v_x(t)^2 \tag{7}$$

The Volland-Stern electric field (ε) is calculated using the x-component of the solar wind velocity and the z-component of the IMF. The dynamic pressure (P_{dyn}) is calculated using the solar wind density and the x-component of the solar wind velocity. The empirically determined values are α (in units of [nT/hr]/[mV/m]), τ (in units of hrs), E (in units of mV/m), b (in units of nT/(eV/cm^3)$^{1/2}$), and c (in units of nT). *Fenrich and Luhmann* [3] and *O'Brien and McPherron* [4] based their empirical models on these same equations. Table 1 lists the values used for each of these models.

Table 1. *Empirical values for models*

Name	*Burton et al.* [2]	*Fenrich and Luhmann* [3]	*O'Brien and McPherron* [4]
α ([nT/hr]/[mV/m])	-5.4	$-4.32\left(P_{dyn}(t)\right)^{1/3}$	-4.4
τ (hours)	7.7	$\begin{array}{ll} 7.7 & v_x(t)B_z(t) \le 4 \\ 3 & v_x(t)B_z(t) > 4 \end{array}$	$2.4\left(\frac{9.74}{4.69+v_x(t)B_z(t)}\right)$
E (mV/m)	0.5	0.5	0.5
b (nT/(eV/cm^3)$^{1/2}$)	0.2	0.158	0.0726
c (nT)	20	20	11

If the solar wind and IMF data used are those measured at the L1 point between the Sun and Earth, these models can be used to forecast the next hourly value for the *Dst* index. The models can be run either by simulation or extrapolation. In simulation, only the sentinel solar wind and IMF data is used to calculate the *Dst* values and change in *Dst* during the time step. In extrapolation, the nowcast *Dst* value measured for a particular hour is substituted for the previous *Dst* value.

Two other forecast models will be compared. *Lundstedt et al.* [5] uses a neural network with solar wind and IMF inputs to generate their forecast in simulation mode, and *Temerin and Li* [6] uses a complicated empirical model with approximately 100 free parameters to generate their forecast in simulation mode.

4. THE UKF FORECAST MODEL

The Kalman filter will be used to generate a forecast for *Dst* by extrapolation. The basic steps in a Kalman filter are: 1. the state vector and covariance from the current time step are passed through a state function that translates the values to the next time step creating an "a priori" state vector and covariance, 2. the "a priori" state vector and covariance are used in a measurement function that translates the values to a corresponding predicted measurement and covariance, 3. the predicted measurements and covariance are then compared to the actual measurements and covariance at that time step and this difference along with the so-called "Kalman gain" are used to adjust the values in the a priori state vector and covariance to an "a posteriori" state vector and covariance, and 4. this a posteriori state vector and covariance are then used at the start of the next step. The predicted measurement in step 2 can be used as a forecast value and repeated use of the state and measurement functions at this point in the Kalman filter cycle can create forecasts any number of time steps into the future for the current step.

In a regular Kalman filter, the state function and measurement function must be linear. Various methods have been employed to extend the Kalman filter for use with nonlinear functions. We will use the Unscented Kalman Filter (UKF) (also called the Sigma-Point Kalman Filter) that employs the unscented transform [7]. The UKF combines Kalman filtering, the optimal filter for estimating linear systems, with the unscented transform, which uses deterministic sampling to estimate the state and covariance of the system through a nonlinear function. The UKF has seen extensive use in spacecraft attitude determination [8,9,10,11]. In this study, we use the nomenclature of [9] and set the UKF tuning parameters to $\alpha = 1, \beta = 0$ and $\kappa = 0$.

The key to using the UKF as a forecast model will be in creating a state vector ($\hat{x}_k$) and covariance (P_k), a state function ($f(\hat{x}_k, w_k)$) and a measurement function ($h(\hat{x}_k, v_k)$). In the model described below, we use an n×1 state vector given by

$$\hat{x}_k^+ = \vec{c}_k^+ \tag{8}$$

where $\vec{c}_k^+$ is a vector of parameters to be used in the measurement function. The noiseless state function used is

$$\hat{x}_{k+1} = f(\hat{x}_k, 0) = \hat{x}_k \tag{9}$$

which simply means the parameters in the state vector are assumed to be constant within the time step. The noiseless measurement function used is:

$$\tilde{y}_k = h(\hat{x}_k, 0) = \begin{pmatrix} \frac{2-1/\tau}{2+1/\tau}\left(Dst_{k-1} - (x_5)_k\, n_{k-1} (v_x)_{k-1}^2 + (x_6)_k\right) + \\ \frac{\alpha}{2+1/\tau}\left[(v_x)_{k-1}(B_z)_{k-1} + (v_x)_k (B_z)_k - 2(x_7)_k\right] \end{pmatrix} + (x_5)_k\, n_k (v_x)_k^2 - (x_6)_k \tag{10}$$

where

$$\alpha = (x_1)_k \left(\frac{n_{k-1}(v_x)_{k-1}^2 + n_k (v_x)_k^2}{2} \right)^{1/3} \tag{11}$$

$$\tau = (x_2)_k \exp\left(\frac{(x_3)_k}{(x_4)_k + \max(0, (v_x)_k (B_z)_k)} \right) \tag{12}$$

Eq. 10 is based on the general formula from [2], while Eq. 11 uses the formula for α as in [3] and Eq. 12 uses the formula for τ as in [4]. In all cases, the empirical values have been replaced by a state vector parameter for a total of seven.

The +1hr forecast at step *k* is $\hat{y}_k$ in the nomenclature of the UKF. Additional forecasts (for +2hr, +3hr, etc…) at step *k* are accomplished by using Equation 9 and 10 iteratively at that point in the UKF cycle. The values of the solar wind and IMF values used in Eq. 10 for these extended forecasts were kept constant.

In this study, the initial state was set to values consistent with Table 1. The components of the covariance matrix associated with the seven parameters are initially set high to allow the UKF room to adjust them accordingly.

The solar wind and IMF hourly data were tabulated using the Level 2 On-line data archives at the Advanced Composition Explorer (ACE) website (http://www.srl.caltech.edu/ACE/ASC/level2/index.html). Any missing hourly ACE data was replaced with the last valid value for that quantity. All the data was processed with the UKF multiple times using the final state vector of the current iteration as the initial state vector of the next iteration until the resulting linear correlation coefficient from one iteration to the next remained essentially constant. In this way, the final iteration starts with parameter values close to their optimal values. The UKF model performance is measured from this final iteration. The other models were analyzed using the same set of data.

Fig. 4 reproduces Fig 3b for the 1998 to 2006 data and compares the performance of simple persistence to the UKF forecast. It is clear the UKF model improves the RMSE overall and for storm-time *Dst* values.

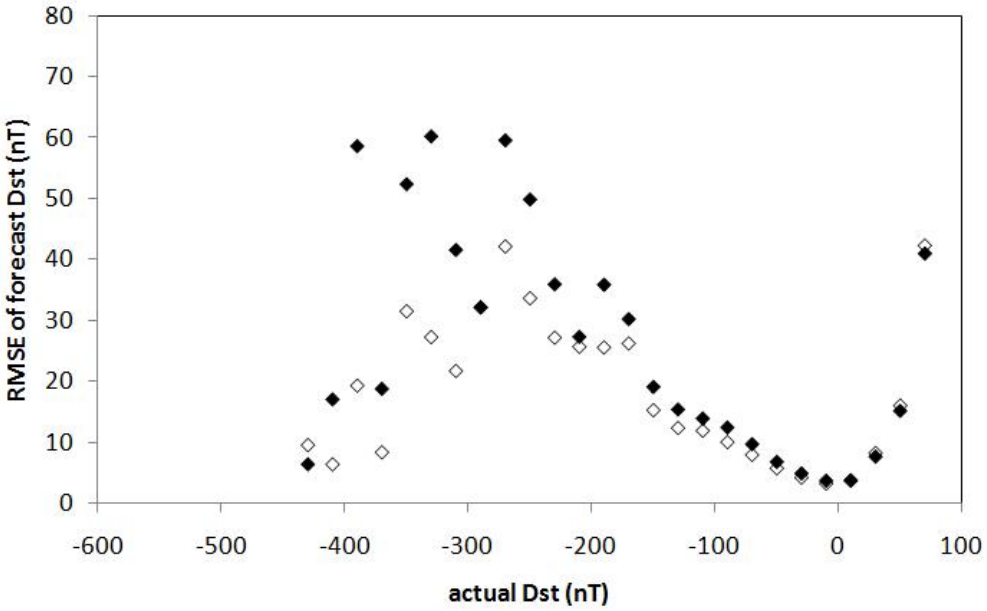

Figure 4 – Root-mean square error as function of actual Dst for simple persistence (filled diamonds) and UKF model (open diamonds).

Table 2 and Fig. 5 compare the performance of all the various forecast models to simple persistence. The UKF model slightly outperforms the next best model (*O'Brien and McPherron* run in extrapolation mode). The results for *Temerin and Li* are those from their paper.

Table 3. 3-hr forecast correlation coefficient for simple persistence model

Time period	r	RMSE (nT)	SS
Simple persistence (ext)	0.978	5.454	0.000
UKF (ext)	0.986	4.368	0.626
Burton et al. (sim)	0.760	18.878	0.061
Burton et al. (ext)	0.982	4.914	0.600
Fenrich and Luhmann (sim)	0.697	21.851	0.170
Fenrich and Luhmann (ext)	0.964	7.064	0.617
O'Brien and McPherron (sim)	0.833	14.739	0.033
O'Brien and McPherron (ext)	0.985	4.440	0.604
Lundstedt et al. (sim)	0.842	14.662	0.429
Temerin and Li (sim)	0.958	6.875	

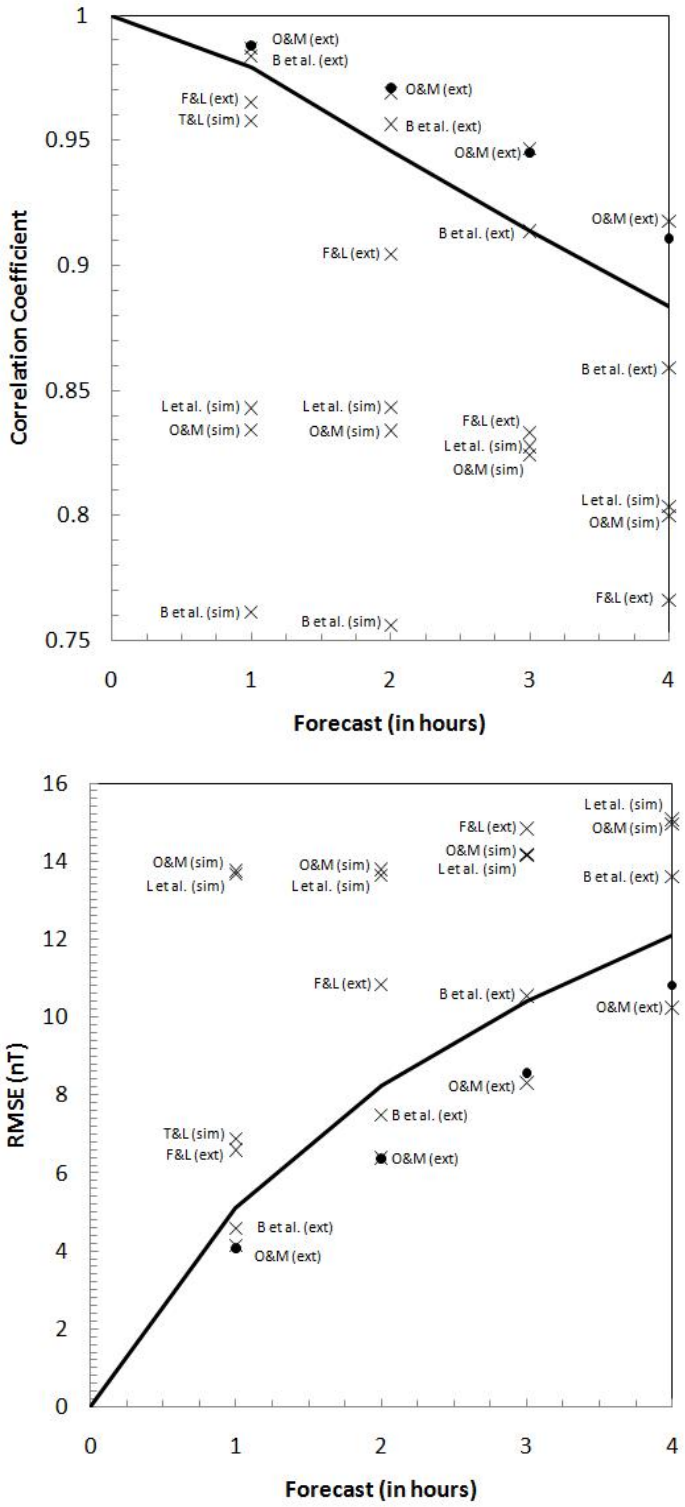

Figure 5 –Model x-hour ahead (a) correlation coefficient and (b) RMSE as a function of x (forecast in hours). Simple persistence model (line), and UKF model (filled ciricles) compared to all previous models run in simulation and extrapolation (X's and labeled).

5. CONCLUSIONS

The disturbed storm time (*Dst*) index displays a high degree of persistence. Once again, the unscented Kalman filter (UKF) was used as the engine behind a forecast model and performs slightly better than all previously published forecast models.

The utility of using the UKF as the engine behind a forecast model for geomagnetic indices is now well established. The possibility of incorporating a host of other inputs to the model and exploring the use of other state and measurement functions is straight forward, and so improvement in performance is achievable.

6. ACKNOWLEDGEMENTS

This work was accomplished as a Colorado Professional Resources, LLC employee under subcontract JT515 to TEAS contract FA9200-07-C-0006 on task order TEASV-08-1204. The author would also like to acknowledge valuable discussions with Dr. Moriba Jah (Director, Advanced Sciences and Technology Research Institute for Astrodynamics (ASTRIA), AFRL, Albuquerque, New Mexico, USA) and Mr. Kevin Scro (Defense Meteorological Satellite Program Systems Group Technical Director, Peterson AFB, Colorado Springs, Colorado, USA).

7. REFERENCES

1. Wetterer, C. J., M. K. Jah, and K. Scro (2010), Kp Forecast Model Using Unscented Kalman Filtering, *11th Advanced Maui Optical and Space Surveillance Technologies (AMOS) Conference*, [Maui Economic Development Board], *http://www.amostech.com/TechnicalPapers/2010/Modeling/Wetterer.pdf*

2. Burton, R. K., R. L. McPherron, and C. T. Russell (1975), An empirical relationship between interplanetary conditions and Dst, J. Geophys. Res., 80, 4204.

3. Fenrich, F.R. and J.G. Luhmann (1998), Geomagnetic response to magnetic clouds of different polarity, *Geophysical Research Letters*, 25(15), 2999-3002

4. O'Brien, T.P. and R.L. McPherron (2000), Forecasting the ring current index Dst in real time, Journal of Atmospheric and Solar-Terrestrial Physics, Vol. 62, Issue 14, 1295-1299

5. Lundstedt, H., H. Gleisner, and P. Wintoft (2002), Operational forecasts of the geomagnetic Dst index, Geophysical Research Letters, Vol. 29, No. 24, 2181, doi:10.1029/2002GL016151

6. Temerin, M., and X. Li (2006), Dst model for 1995-2002, Journal of Geophysical Research, Vol. 111, A04221, doi:10.1029/2005JA011257

7. Julier, S. G., and J. K. Uhlmann (1997), A new extension of the Kalman filter to nonlinear systems, *Proceedings of SPIE: The International Society for Optical Engineers*, Vol. 3068, 182-193

8. van der Merwe, R., and E.A Wan (2001), The square root unscented Kalman filter for state and parameter-estimation, *2001 IEEE International Conference on Acoustics, Speech, and Signal Processing*, Vol. 6, 3461-3464

9. Crassidis, J. L., and F. L. Markley (2003), Unscented filtering for spacecraft attitude estimation, *Journal of Guidance, Control, and Dynamics*, Vol. 26, No. 4, pp. 536-542

10. Jah, M. K., Lisano, M. E., II, Born, G.H., and Axelrad, P. (2008), Mars aerobraking spacecraft state estimation by processing inertial measurement unit data, *Journal of Guidance, Control, and Dynamics*, Vol. 31, No. 6, pp. 1802-1813

11. Wetterer, C. J., and M. K. Jah (2009), Attitude estimation from light curves, *Journal of Guidance, Control, and Dynamics*, Vol. 32, No. 5, pp. 1648-1651